EUROPEAN SYNCHROTRON RADIATION FACILITY

INSTALLATION EUROPEENNE DE RAYONNEMENT SYNCHROTRON

Experiment Report Form

	Experiment title: Ligament Shielding and Crack Bridging in Stress Corrosion and Brittle Fracture of Metals	**Experiment number**: ME451
Beamline: ID15	**Date Of Experiment**: From: 4 Dec 02 To: 7 Dec 02	**Date of report**: Dec 03
Shifts:9	**Local contact(s)**: T. Burslaps, Sandrine SCHLUTIG (e-mail: schlutig@esrf.fr)	*Received at ESRF:*

Names and affiliations of applicants (* indicates experimentalists):

[1]T.J. Marrow*

[1]P. Withers

[1]A. Steuwer*

[1]D. Engelberg*

Manchester Materials Science Centre, UMIST and University of Manchester, UK

Report:

Aim To resolve for the first time the crack-tip stress intensity field for a material that fails by stress corrosion cracking and to assess the crack tip bridging caused by uncracked ductile ligaments.

Background

The high strength, toughness and corrosion resistance of ferrite-matrix duplex stainless steels are required in the offshore oil and gas industry. Stress corrosion cracking failures in duplex stainless steels are uncommon, but are particularly expensive when offshore components require repair or recovery from the sea-bed. It is therefore necessary to identify microstructures that are susceptible to brittle fracture and stress corrosion crack propagation and which may, particularly in the anisotropic microstructures of large forgings, permit easy and fast crack growth. Failures have occurred under cathodic protection.

Fracture studies have been conducted in age-hardened duplex stainless steel, which in the embrittled condition exhibits stress corrosion cracking under cathodic conditions [1-3]. Values of the threshold stress intensity for stress corrosion, K_{1SCC}, measured by crack arrest, are widely scattered due to bridging ligaments behind the crack tip and show R-curve behaviour [Figure 1]. Bridging ligaments occur on two length scales. Small-scale bridging ligaments are observed in a crack tip process zone that comprises cleaved ferrite bridged by ductile austenite. This zone is up to 5 mm long and spans the width of the crack [Figure 2]. Longer narrow ligaments, typically 5-10 mm in length, are the result of random branching and forking of the crack plane, and these can also act to shield the crack tip.

Branching is a random process influenced by the specimen geometry, and the worst-case defect in a structure must be assumed to propagate without branching or forking. The lower bound value of K_{1SCC} is therefore most important, and gives the intrinsic resistance of the material to crack propagation. This is determined by austenite grain bridging in the crack tip process zone, which shields the crack tip from the applied stress. The magnitude of shielding due to bridging is expected to depend on microstructure texture, and bridging has a greater effect on the behaviour of short cracks (i.e. less than few mm in length) than longer cracks. We aimed to demonstrate that synchrotron measurements could be used to characterise the bridging stress distribution in the crack tip process zone in bulk specimens of duplex stainless steel, and thus quantify the shielding contribution.

Experimental method

All tests were performed using a bolt-loaded wedge opening load (WOL) side-grooved specimen with a central thickness of approximately 10 mm (full thickness 25 mm, height 60 mm, width 80 mm). The specimen had been fatigue pre-cracked and tested at –900mV SCE in pH 7.5 saturated NaCl solution (3.5wt% in water) at a stress intensity factor of 60 MPa√m for 2 weeks to produce a stress corrosion crack with a surface length of approximately 3 mm. The load was applied to the specimen using a bolt [Figure 3]. The applied load was determined by in-situ measurement of the crack mouth opening displacement (clip gauge), which had been previously calibrated for the specimen. From this, the applied stress intensity factor during the experiment could be calculated.

The selected beam energy was 100 keV, which gave diffraction peaks in both ferrite and austenite at low angle (~3.5º), effectively measuring the elastic strains in transmission through the specimen. The region around the crack was mapped with a gauge volume defined by the 150 x 150 µm incident beam geometry at $2\theta = 3.5°$. This gave a gauge volume with a width of approximately 3mm perpendicular to the specimen thickness. The step size in the map was 0.1 mm, with a typical mapping duration of 8 hours for the count time of 15 seconds. Strain measurements were made with the specimen under zero load, and at various levels of load up to 60 MPa√m. Compliance measurements with unloading were used to demonstrate that no crack growth or plasticity was introduced during the strain-scanning experiment.

The results were prepared using a Pawley refinement approach, using the software package GSAS Pawley-type extraction model. The collected spectra were thus transformed to an artificial, reciprocal scale, essentially equivalent to that of time-of-flight, and then stored in GSAS RALF format using logarithmic rebinning, which then allows the use of the asymmetric TOF neutron diffraction peak profiles in GSAS.

After the strain-scanning experiment, the sample was sectioned perpendicular to the crack plane. A series of metallographic sections were prepared within the strain scanned gauge volume at intervals of 0.5 mm to determine the crack shape and extent of the bridging zone. Alignment to 0.25 mm between the strain scanning and the metallography was achieved by first marking photographic film on the specimen with the beam, followed by hole-punch and drilling reference holes with 0.5 mm diameter through the specimen thickness.

The elastic strains in the austenite and ferrite, calculated from the d-spacing, were converted to stress by assuming that the average strain remote from the crack was zero, and using an elastic modulus of 200 GPa for both ferrite and austenite. The positive correction for both phases was approximately 2200µstrain. The stress map for austenite [Figure 4] shows raised stress in the wake of the crack tip, but does not clearly identify the crack or its tip. This is probably due to the relatively small number of grains in the diffracting condition within the gauge volume, and the small volume of highly stressed grains at the crack tip or in the crack wake. The stresses in the ferrite have a similar pattern. The stresses are do not vary significantly perpendicular to the crack. The stress (and standard deviation) averaged over a line within the stress map, perpendicular to the crack plane was calculated for both ferrite and austenite, and is given in Figure 5. The bridging zone is indicated by the positions of the crack tip and the location of the first bridge (measured from the crack mouth). Stresses in the ferrite and austenite are similar, and are clearly raised within the bridged zone when the crack is loaded. This implies that there is traction in the crack wake, due to bridging, which restricts the opening of the crack. This would shield the crack tip from the applied load, and increase resistance to crack propagation. Metallography confirmed the presence of small scale bridging [Figure 2].

The average stress in the bridging zone is 400MPa [Figure 5]. The predicted effect for a simple shielding model with an average stress of 400MPs is shown in Figure 1, giving reasonable agreement with the data. Work is currently in progress to develop a more sophisticated calculation, using the weight function for the specimen geometry, to more accurately evaluate the effect of the measured bridging stresses.

Summary
To the authors knowledge, these observations are the first direct measurement of bridging stresses in the wake of a stress corrosion crack. The magnitude of the stresses is sufficient to cause the observed R-curve behaviour. Work is now in progress to determine the mechanism of failure of the bridges in the crack wake, which enables propagation of the crack above K_{1SCC}.

Figures

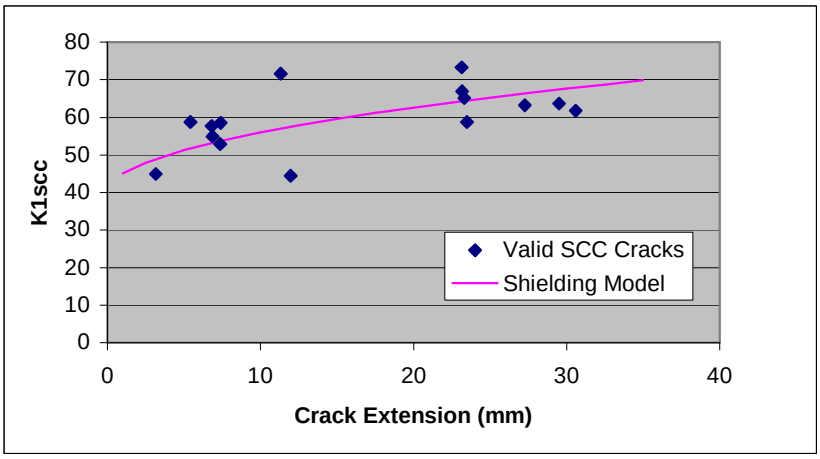

Figure 1: R-curve behaviour for stress corrosion cracking in duplex stainless steel at –900mV in 3.5wt% NaCl.

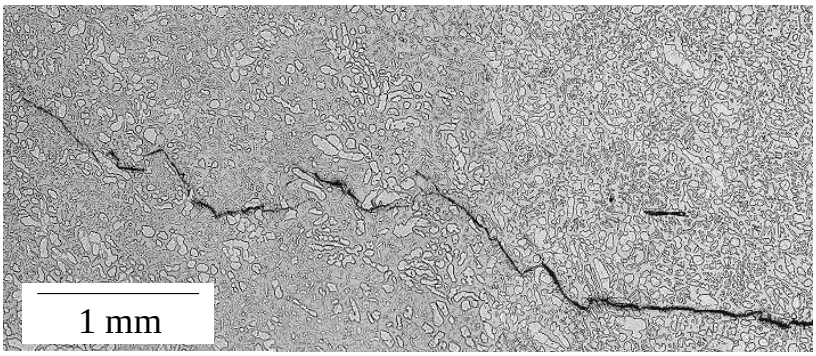

Figure 2: Bridged stress corrosion cracking in duplex stainless steel at –900mV in 3.5wt% NaCl

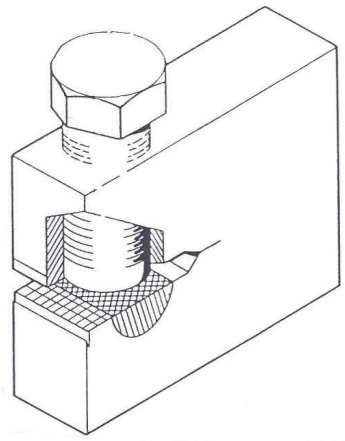

Figure 3: Bolt loaded specimen.

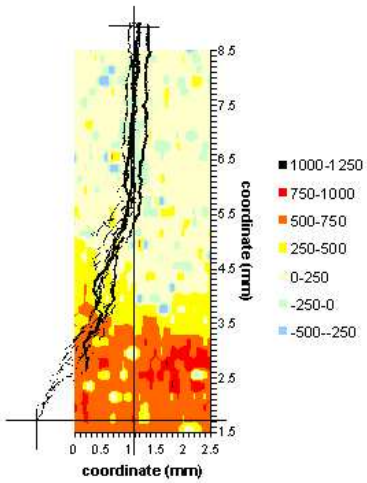

Figure 4: Stress map for austenite (calculated from normalised strains) superposed with the cracks profiles from serial sectioning in the gauge volume.

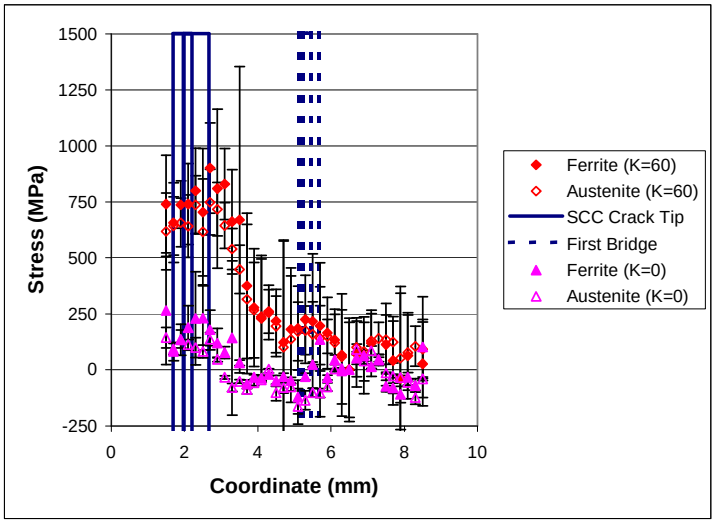

Figure 5: Average stress across crack in the unloaded (K=0 MP√m) and loaded (K=60 MP√m) in ferrite and austenite. The region of bridging lies between the position of the crack tip and the first bridge, which is marked for all the metallographic sections through the gauge volume.

References

1. T.J. Marrow, S. Kim and J-T Oh. *The effect of microstructure on brittle fracture and stress corrosion cracking in duplex stainless steel.* Stainless Steel World 99 (The Hague, November 1999).
2. S. Kim and T.J. Marrow. *Application of electron backscattered diffraction to cleavage fracture in duplex stainless steel.* Scripta Materialia, 40, (1999), 1395-1400
3. T.J. Marrow, A.O. Humphreys and M. Strangwood. *The crack initiation toughness for brittle fracture of super duplex stainless steel.* Fatigue and Fracture of Engineering Materials and Structures, 20, (1997), 1005-1014.